How do cicadas emerge together? Thermophysical aspects of their collective decision-making

Raymond E. Goldstein [1,*] Robert L. Jack [1,2,†] and Adriana I. Pesci [1,‡]

[1] *Department of Applied Mathematics and Theoretical Physics, Centre for Mathematical Sciences, University of Cambridge, Wilberforce Road, Cambridge CB3 0WA, United Kingdom*

[2] *Yusuf Hamied Department of Chemistry, University of Cambridge, Lensfield Road, Cambridge CB2 1EW, United Kingdom*

Periodical cicadas exhibit life cycles with durations of 13 or 17 years, and it is now accepted that large prime cycles arose to avoid synchrony with predators. Less well explored is *how*, in the face of intrinsic biological and environmental noise, insects within a brood emerge together in large successive swarms from underground during springtime warming. Here, we consider the decision-making process of underground cicadas experiencing random, spatially correlated thermal microclimates such as those in nature. Introducing short-range communication between insects leads to an Ising model of consensus building with a quenched, spatially correlated random magnetic field and annealed site dilution, which displays the kinds of collective swarms seen in nature. These results highlight the need for fieldwork to quantify the spatial fluctuations in thermal microclimates and their relationship to the spatiotemporal dynamics of swarm emergence.

Introduction. Vast, coherent swarms of insects have been recorded by humanity since at least biblical times [1], and yet we do not understand how this coherence arises. One of many such examples of coherence is found in the synchronized springtime emergence from underground of cicadas of the genus *Magicicada*, which has been the subject of detailed entomological field studies for over a century [2]. From work documenting the geographic distribution of emergences of 13- or 17-yr species [3], to studies of their underground developmental stages [4–6], it is understood that any given brood (group emerging in a particular year) exhibits two types of synchrony: (i) Essentially all members emerge precisely in year 13 or 17, and (ii) they do so when the local soil temperature crosses a threshold in that particular year [5].

These observations motivated numerous studies in theoretical population biology to understand the reasons *why* large prime number periods have been selected by evolution, but far fewer studies explaining *how* the two levels of synchrony are achieved. For prime number selection, the hypothesis [7,8] that limited environmental carrying capacity and predation pressure are responsible was first captured in a mathematical model by Hoppensteadt and Keller [9]. Later models elucidated mechanisms by which single broods occupy disjoint areas [10–12].

These studies do not address how a brood recognizes that it is year 17 (and not, say, 16) and then emerges in a sequence

of vast swarms throughout several weeks. The 17 years spent underground by nymphs are divided into five developmental stages (5 *instars*), the duration of which exhibits considerable dispersion (Fig. 1). Despite this spread, cicadas accurately keep track of the passage of years while underground. It is known that after hatching the nymphs burrow below ground and obtain nutrients from the xylem in tree roots [13]. They therefore experience the annual seasonal cycles of the trees, as shown by Karban *et al.* [14], who artificially altered the cycles in year 15 to provoke an early emergence, proving that cicadas count cycles and not the passage of time itself. It is unclear how such accurate counting occurs, but it has been suggested [2] that it could involve epigenetic modifications of the kind observed in long-lived plants such as bamboo [15]. Similar issues arise in flowering plants, which must experience a minimum number of cold days in order to flower [16].

Surprisingly, there is no systematic field data in existence on the spatiotemporal dynamics of swarms themselves. However, the issue of swarm emergence in a given year was studied by Heath [5], who found that the day d_c of emergence of 17-yr cicadas in any given location is strongly correlated with the local soil temperature reaching the threshold $T_c \simeq 18\,°C$. This conclusion raises the question of how cicadas can emerge in great swarms in spite of spatially varying microclimates, their own distribution of body temperatures on emergence [5], and the inherent imprecision of temperature sensing by the cicadas themselves. Here, we develop the hypothesis that the thermally triggered synchronized emergence of cicadas arises in part from short-ranged communication between nearby underground nymphs that allows for collective decision-making. That cicadas are capable of collective behavior by means of communication is evidenced by their acoustically synchronized above-ground choruses [17,18]. While choruses occur soon after emergence, and it is plausible that the ability to hear underground noise [19] is present earlier, acoustical coupling is but one of several communication mechanisms that may be

*R.E.Goldstein@damtp.cam.ac.uk

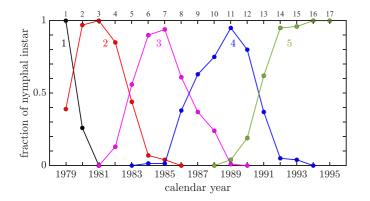†rlj22@cam.ac.uk

‡A.I.Pesci@damtp.cam.ac.uk

FIG. 1. Proportion of cicadas in the 5 instars as a function of time, for one brood. Adapted from Ref. [6].

operating, and our analysis does not depend on the specific means. Collective behavior via communication [20] is found in many contexts: bacterial quorum sensing [21], ant foraging [22–24], and bird flocking [25].

As in other studies of collective behavior [26–28], our model of decision-making is a random-field Ising model (RFIM) [29,30], in which quenched randomness arises from microclimates and spins represent the decision. We introduce additional site occupancy variables in order to interpret the simultaneous flipping of many spins ("avalanches") as swarms. Numerical studies of this model produce swarms such as those found in nature, and highlight important directions for future fieldwork.

Thermobiology of burrowing nymphs. Newly hatched nymphs burrow to a depth $z_b \sim 30$ cm that is thought from observations [5] to isolate them from strong diurnal temperature fluctuations. To put this on a quantitative basis, we consider the temperature variations in Ohio, where there is a wealth of data on cicada emergence [5]. Figure 2(a) shows the average daily low and high temperatures at 2 m above ground in Columbus, Ohio [31]. We take these to define a suitable average boundary condition $T(0, d)$ for the subsurface temperature field $T(z, d)$ with z increasing downward and d is time measured in days. These data can be represented by a superposition of annual (a) and daily (d) cycles,

$$T(0, d) = \bar{T} - \Delta_a \cos(2\pi \nu_a d') - \Delta_d \cos(2\pi \nu_d d'), \quad (1)$$

where $d' = d - d_0$, with $d_0 \simeq 20$ (January 20th) being the day of lowest temperatures, with annual frequency $\nu_a = (1/365)$ day^{-1}, daily frequency $\nu_d = 1$ day^{-1}, $\bar{T} = 12.1\,°$C, $\Delta_a = 12.4\,°$C, and $\Delta_d = 4.8\,°$C. We assume the underground temperature $T(z, d)$ obeys the diffusion equation $\partial_d T = D\partial_{zz}T$, for which typical values of the thermal diffusion constant D are in the range $(0.8–10) \times 10^{-7}$ m^2/s [32]. We adopt the middle of this range $D \sim 5 \times 10^{-7}$ m^2/s $= 432$ cm^2/day.

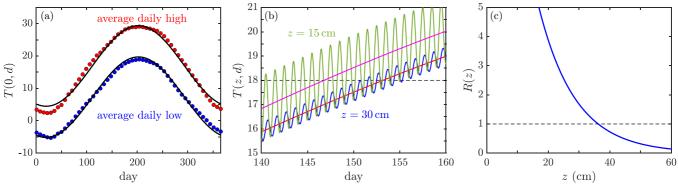Introducing the scaled time $t = \nu_d d'$ and $\epsilon = \nu_a/\nu_d$, Eq. (1) implies the subsurface temperature field

$$T(z, t) = \bar{T} - \Delta_a e^{-z/\ell_a} \cos(z/\ell_a - 2\pi\epsilon t)$$
$$- \Delta_d e^{-z/\ell_d} \cos(z/\ell_d - 2\pi t)$$
$$\equiv \bar{T} - T_a(z, \epsilon t) - T_d(z, t), \quad (2)$$

with penetration lengths $\ell_i = \sqrt{D/\pi\nu_i}$ for $i = a, d$, with values $\ell_a \sim 224$ cm and $\ell_d \sim 12$ cm, respectively. Examining the subsurface temperature field at different depths, as in Fig. 2(b), we see that at $z = 15$ cm the within-day oscillations are very large compared to the change in the mean between successive days, whereas at $z = 30$ cm the two are comparable. To quantify the relative size of these contributions we define $R(z)$ as the ratio between the root-mean-square daily fluctuations in T_d and the change in the annual trend T_a over one day. Since $\epsilon \ll 1$, that change is approximately $(\partial/\partial t)T_a(z, \epsilon t)$, yielding

$$R(z, t) = -\frac{\Delta_d\, e^{-z\left(\frac{1}{\ell_d} - \frac{1}{\ell_a}\right)}}{2^{3/2}\pi\epsilon\,\Delta_a \sin[z/\ell_a - 2\pi\epsilon t]}. \quad (3)$$

Shown in Fig. 2(c), this ratio decreases with depth, crossing below unity at the burrowing depth $z_b \sim 30$ cm. While fluctuations are attenuated relative to the surface, the thermal noise there is comparable to the signal, and thus crossing of the temperature threshold cannot be synchronously determined by a population of nymphs, buried at a distribution of depths, acting independently.

Microclimates and coarse graining. The above does not account for *lateral* variations in temperature with elevation, tree cover, and solar exposure, which determine the local *microclimate*. As Heath showed, the days of cicada emergences varied with location in a hilly landscape as shown in Fig. 3(a) [5]. Sunny, sparsely forested south-facing slopes

FIG. 2. Temperature variations. (a) Daily average low and high surface temperatures in Columbus, Ohio, subsampled weekly, and daily extrema of two-mode approximation (1) (black). (b) Theoretical average subsurface temperature at two depths near $T_c = 18\,°$C. (c) Noise ratio R in (3) vs depth near the crossing day.
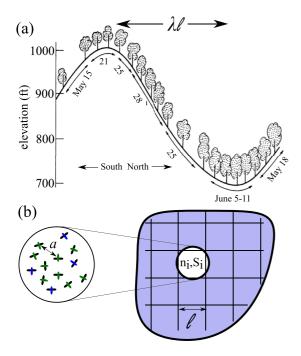
FIG. 3. Lateral temperature variations. (a) Topography of an Ohio forest, indicating forest density and dates of cicada emergences. Adapted from Ref. [5]. (b) Region of burrowing nymphs, with typical spacing a, coarse grained on the scale ℓ. Microclimates are correlated on the scale $\lambda \ell$.

have the earliest swarms, with successive swarms typically separated by a gap of several days, disproving the simplistic view that all cicadas in a brood emerge at once within a few days; the entire process within an emergence year may take a month.

While a full description of microclimate requires accounting for topography, solar exposure, and vegetation, we argue that the net effect of these contributions is that nymphs experience a *quenched, spatially correlated random temperature field*. From our analysis of underground temperatures, we identify the annual penetration length ℓ_a as the smallest scale of that random field which, therefore, serves as a coarse-graining length ℓ. The area density n of cicadas can reach $10^6/\text{acre} \sim 250/\text{m}^2$ [33], with average distance $a \sim 1/\sqrt{n}$ between nymphs as small as 5–10 cm $\ll \ell \sim 2$ m. We adopt the coarse-grained representation of the population density $n(\mathbf{r})$ at point $\mathbf{r}$ in Fig. 3(b), where each subgroup b_i of area ℓ^2 is associated to a site on a square lattice at location $\mathbf{x}_i = \mathbf{r}_i/\ell \in \mathbb{Z}^2$ and, as in a lattice-gas description, is assigned an occupation variable n_i denoting if it is empty (0) or occupied (1).

The burrowing depth of nymphs, and the separation of scales $a \ll \ell$ suggest that a natural model of the thermal environment of cicadas involves a two-dimensional temperature field $\tau(\mathbf{x}_i, t) = \tau_m(t) + \tilde{\tau}_f(\mathbf{x}_i)$, partitioned into a slowly rising mean $\tau_m(t)$ obtained from $T(z_b, t)$ in (2) by averaging over the fast daily oscillations, and a term $\tilde{\tau}_f(\mathbf{x}_i)$ that encodes the fluctuations in the local microclimate. Shifting the origin of temperature to be T_c, near the crossing day we may write $\tau_m(t) \simeq \tilde{\alpha}(t - t_c)$, where $\tilde{\alpha} \simeq 0.15\,^\circ\text{C}$. We assume that $\tilde{\tau}_f(\mathbf{x})$ is a Gaussian random field with zero mean and some

two-point correlation

$$C(|\mathbf{x}_i - \mathbf{x}_j|) = \langle \tilde{\tau}_f(\mathbf{x}_i)\tilde{\tau}_f(\mathbf{x}_j)\rangle. \tag{4}$$

In practice we assume an exponential correlation $C = \sigma^2 e^{-|\mathbf{x}_i - \mathbf{x}_j|/\lambda}$ with a single (scaled) length λ, where σ is the standard deviation of the local field, in the range $\sim$1–3 $^\circ$C. From the topography of Fig. 3(a) and contour maps of the regions studied by Heath, we deduce $\lambda \sim 50$.

Model of decision-making. To complete the model by allowing for nymph communication, we introduce a second variable at each site: a spinlike scalar $S_i(t)$ that characterizes the binary choice at a given time, to remain underground (-1) or to emerge ($+1$). The decision of group b_i to emerge is determined by the local temperature and the behavior of other groups in the neighborhood V_i (the $q = 8$ nearest and next-nearest neighbors of site i) via the field $\mathcal{H}_i(t) = \mathcal{J}_i(t) + \tau(\mathbf{x}_i, t)/\sigma$, where the temperature has been nondimensionalized by σ, and

$$\mathcal{J}_i(t) = J \sum_{j \in V_i} n_j(t)S_j(t), \tag{5}$$

in which we adopt the simplest model with a single coupling J throughout the neighborhood. Hence

$$\mathcal{H}_i(t) = \alpha(t - t_c) + \tau_f(\mathbf{x}_i) + \mathcal{J}_i(t), \tag{6}$$

where $\alpha = \tilde{\alpha}/\sigma$, and $\tau_f = \tilde{\tau}_f/\sigma$ has unit variance. As in previous models of collective decision-making [26,27], the decision of S_i to flip from -1 to $+1$ occurs when $\mathcal{H}_i$ becomes positive, as in the "zero-temperature" limit of the RFIM approach. When $J = 0$, each spin flips to $+1$ when its local temperature field crosses the threshold. When $J > 0$, a subgroup's decision to emerge is reinforced by occupied neighboring sites that have flipped, a feature that leads to swarms. $\mathcal{H}_i$ plays the same role as the local field in a spin model of magnetization; with the occupation variables n_i, the system is a random field Ising model (RFIM) with annealed site dilution. In most studies of the RFIM the random field is independent from site to site, but here the microclimates are correlated on scales large compared to the lattice spacing.

The dynamics of decision-making by subgroups is modeled as a discrete-time process in which state variables are updated daily, without resolving the behavior within each day. In numerical studies, we start at $t < t_c$ with full occupancy ($n_i = 1, \forall i$), and with all subgroups choosing to remain underground ($S_i = -1, \forall i$). On each day we iteratively update the spins by the rule $S_i^{k+1} = \text{sgn}[\mathcal{H}_i^k]$, where $k = 1, 2, \dots$ labels iterations, until no more spins flip to $+1$. We call a *swarm* the set $\mathcal{A}(t)$ of spins that have flipped from -1 to $+1$ on a given day. The occupancy variables of sites in $\mathcal{A}(t)$ are set to zero when the updating rule is complete for that day. The process continues on successive days until the entire lattice is empty.

Numerical studies. The model (6) has three dimensionless parameters (α, J, λ) and the dimensionless system size L [34]. Since the tails of τ_f determine the first and last swarms, some 95% of the cicadas emerge over a period of $4/\alpha$ days, during which time the mean temperature sweeps from -2σ to $+2\sigma$ of the random field; setting $\alpha = 0.3$ spreads swarms over the realistic time of $\sim$14 days. Consider first the effect of the coupling J at fixed λ. Figure 4(a) shows a realization of $\tau_f(\mathbf{x})$ with $\lambda = 30$, within which are correlated local
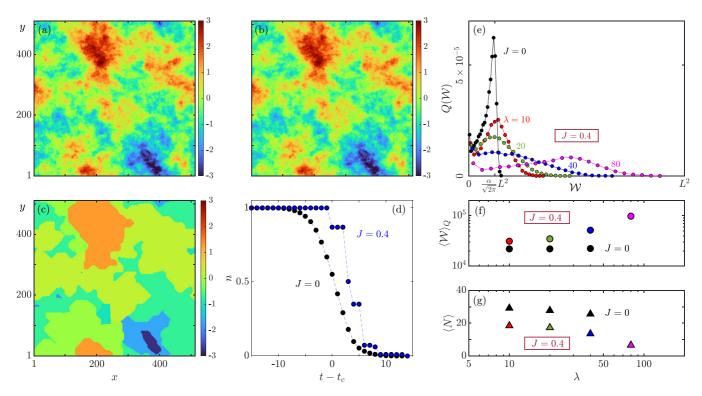
FIG. 4. Numerical results with $L = 512$. (a) Realization of the random field $\tau_f(\mathbf{x})$. (b), (c) Composite plots of swarms for $J = 0$ and $J = 0.4$, respectively, color coded by mean value of τ_f within each swarm, with $\alpha = 0.3$. (d) Occupancy vs time for cases in (b) and (c). [(e)–(g)] Results from averaging over 10^4 realizations of τ_f for $J = 0$ (black) and $J = 0.4$ (colors). (e) Binned swarm size distribution $Q(\mathcal{W})$ for $J = 0$ and for $J = 0.4$ and several values of λ. (f), (g) Average swarm size experienced by a cicada and average number of swarms vs λ. At $J = 0$, the decrease in $\langle N \rangle$ for $\lambda \gtrsim 40$ is a finite-size effect.

"hot spots" and "cold spots" in the landscape: such as sunny hilltops and shaded valleys. If $J = 0$ [Fig. 4(b)], the swarms are composed of those sites whose random field values fall in intervals of size α. As τ_f is Gaussian, the lattice occupancy versus time [Fig. 4(d)] is a discretely sampled error function $\langle n \rangle \approx \text{erfc}[\alpha(t - t_c)/\sqrt{2}]/2$. In contrast, when $J > 0$ [Fig. 4(c)], intercicada coupling produces large coherent domains. Emptying the lattice involves a smaller number of large swarms, which may be separated by time gaps without activity, as in Heath's observations [5]. This picture—of quiescent periods punctuated by large emergence events—resembles the avalanches seen in the conventional RFIM, but the event initiation differs due to the daily resetting of the occupancy variables.

Next, we examine properties of swarms averaged over 10^4 realizations of τ_f, through the distribution $P(\mathcal{W})$ of swarm sizes $\mathcal{W}$, with mean $\langle \mathcal{W} \rangle_P = \sum \mathcal{W} P(\mathcal{W})$ and $Q(\mathcal{W}) = \mathcal{W} P(\mathcal{W})/\langle \mathcal{W} \rangle_P$, the probability that a given cicada emerges in a swarm of size $\mathcal{W}$ [35]. We see in Fig. 4(d) that when $J = 0$ the largest swarms occur near t_c, where from the form of $\langle n \rangle$ above we deduce the maximum average swarm size to be $\sim \alpha L^2/\sqrt{2\pi}$. This sharp cutoff is clearly visible in $Q(\mathcal{W})$ shown in Fig. 4(e). In contrast, when $J = 0.4$ the probability distribution function (pdf) $Q(\mathcal{W})$ broadens with increasing correlation length of the random field, signifying the existence of ever larger swarms. This is further quantified by examining

$\langle \mathcal{W} \rangle_Q = \sum \mathcal{W} Q(\mathcal{W})$), the average size of a swarm in which a given cicada emerges. Figures 4(f) and 4(g) show that beyond $\lambda \sim 20$, the effect of communication ($J > 0$) is that the average swarm size is larger, and the number of swarms depends more strongly on λ. These trends continue for larger J.

We have shown that the statistical physics of collective decision-making, quantitatively based on the thermal physics of local microclimates, reproduces key known features of periodical cicada emergences: compact, large swarms spread over several weeks, with temporal gaps between them. The finite change in temperature per day and the annealed disorder modify some aspects of the standard RFIM behavior. Hence, while our results establish an analogy between insect emergence and random magnets, they also capture some of the differences between these phenomena. Future work should focus on testing the hypothesis of communication between nymphs (e.g., by direct acoustical sampling), quantifying spatial variations in microclimate, and the spatiotemporal dynamics of the emerging swarms themselves. In this regard, organisms with shorter cycles would be of great interest [36].

[1] *The Bible: Authorized King James Version*, edited by R. Carroll and S. Prickett (Oxford University Press, Oxford, UK, 2008).

[2] C. Simon, J. R. Cooley, R. Karban, and T. Sota, Advances in the evolution and ecology of 13- and 17-year periodical cicadas, Annu. Rev. Entomol. **67**, 457 (2022).

[3] C. L. Marlatt, *The Periodical Cicada*, U. S. Department of Agriculture, Bureau of Entomology Bulletin No. 71 (U.S. Government Printing Office, Washington, D.C., 1907).

[4] M. Lloyd and H. S. Dybas, The periodical cicada problem. II. Evolution, Evolution **20**, 466 (1966).

[5] J. E. Heath, Thermal synchronization of emergence in periodical "17-year" cicadas (Homoptera, Cicadidae, Magicicada), Am. Midl. Nat. **80**, 440 (1968).

[6] C. T. Maier, Connecticut is awaiting the return of the periodical cicada, Front. Plant Sci. **48**, 4 (1996).

[7] R. D. Alexander and T. E. Moore, *The Evolutionary Relationships of 17-Year and 13-Year Cicadas, and Three New Species (Homoptera, Cicadidae, Magicicada)*, University of Michigan Museum of Zoology Miscellaneous Publication No. 121 (University of Michigan, Ann Arbor, 1962).

[8] J. White and M. Lloyd, Growth rates of 17 and 13-year periodical cicadas, Am. Midl. Nat. **94**, 127 (1975).

[9] F. C. Hoppensteadt and J. B. Keller, Synchronization of periodical cicada emergences, Science **194**, 335 (1976).

[10] J. C. Blackwood, J. Machta, A. D. Meyer, A. E. Noble, A. Hastings, and A. M. Liebhold, Competition and stragglers as mediators of developmental synchrony in periodical cicadas, Am. Nat. **192**, 479 (2018).

[11] J. Machta, J. C. Blackwood, A. E. Noble, A. M. Liebhold, and A. Hastings, A hybrid model for the population dynamics of periodical cicadas, Bull. Math. Biol. **81**, 1122 (2019).

[12] O. Diekmann and R. Planqué, The winner takes it all: How semelparous insects can become periodical, J. Math. Biol. **80**, 283 (2020).

[13] R. Karban, Experimental removal of 17-year cicada nymphs and growth of host apple trees, J. N. Y. Entomol. Soc. **90**, 74 (1982).

[14] R. Karban, C. A. Black, and S. A. Weinbaum, How 17-year cicadas keep track of time, Ecol. Lett. **3**, 253 (2000).

[15] Z. Zhang, H. Wang, Y. Wang, F. Xi, H. Wang, M. V. Kohnen, P. Gao, W. Wei, K. Chen, X. Liu, Y. Gao, X. Han, K. Hu, H. Zhang, Q. Zhu, Y. Zheng, B. Liu, A. Ahmad, Y.-H. Hsu, S. E. Jacobsen, and L. Gu, Whole-genome characterization of chronological age-associated changes in methylome and circular RNAs in moso bamboo (*Phyllostachys edulis*) from vegetative to floral growth, Plant J. **106**, 435 (2021).

[16] H. Yang, S. Berry, T. S. G. Olsson, M. Hartley, M. Howard, and C. Dean, Distinct phases of polycomb silencing to hold epigenetic memory of cold in *Arabidopsis*, Science **357**, 1142 (2017).

[17] G. Si-Yuan, J. Yu-Liang, Z. Xiao-Xue, and H. Ji-Ping, A possible population-driven phase transition in cicada chorus, Commun. Theor. Phys. **51**, 1055 (2009).

[18] L. W. Sheppard, B. Mechtley, J. A. Walter, and D. C. Reuman, Self-organizing cicada choruses respond to the local sound and light environment, Ecol. Evol. **10**, 4471 (2020).

[19] M. Maeder, X. Guo, F. Neff, D. S. Mathis, and M. M. Gossner, Temporal and spatial dynamics in soil acoustics and their relation to soil animal diversity, PLoS One **17**, e0263618 (2022).

[20] I. D. Couzin, Collective cognition in animal groups, Trends Cogn. Sci. **13**, 36 (2008).

[21] K. H. Nealson, T. Platt, and J. W. Hastings, Cellular control of the synthesis and activity of the bacterial luminescent system, J. Bacteriol. **104**, 313 (1970).

[22] M. Beekman, D. J. T. Sumpter, and F. L. W. Ratnieks, Phase transition between disordered and ordered foraging in Pharaoh's ants, Proc. Natl. Acad. Sci. USA **98**, 9703 (2001).

[23] T. Sasaki, B. Granovskiy, R. P. Mann, D. J. T. Sumpter, and S. C. Pratt, Ant colonies outperform individuals when a sensory discrimination task is difficult but not when it is easy, Proc. Natl. Acad. Sci. USA **110**, 13769 (2013).

[24] O. Feinerman, I. Pinkoviezky, A. Gelblum, E. Fonio, and N. S. Gov, The physics of cooperative transport in groups of ants, Nat. Phys. **14**, 683 (2018).

[25] A. Cavagna, A. Cimarelli, I. Giardina, G. Parisi, R. Santagati, F. Stefanini, and M. Viale, Scale-free correlations in starling flocks, Proc. Natl. Acad. Sci. USA **107**, 11865 (2010).

[26] Q. Michard and J.-P. Bouchaud, Theory of collective opinion shifts: From smooth trends to abrupt swings, Eur. Phys. J. B **47**, 151 (2005).

[27] J.-P. Bouchaud, Crises and collective socio-economic phenomena: Simple models and challenges, J. Stat. Phys. **151**, 567 (2013).

[28] A. T. Hartnett, E. Schertzer, S. A. Levin, and I. D. Couzin, Heterogeneous preference and local nonlinearity in consensus decision making, Phys. Rev. Lett. **116**, 038701 (2016).

[29] J. P. Sethna, K. Dahmen, S. Kartha, J. A. Krumhansl, B. W. Roberts, and J. D. Shore, Hysteresis and hierarchies: Dynamics of disorder-driven first-order phase transformations, Phys. Rev. Lett. **70**, 3347 (1993).

[30] J. P. Sethna, K. A. Dahmen, and O. Perkovic, Random-field Ising models of hysteresis, in *The Science of Hysteresis*, edited by G. Bertotti and I. Mayergoyz (Elsevier, Amsterdam, 2005), Chap. 2.

[31] The data were obtained from https://weatherspark.com/countries/US/OH.

[32] T. Arkhangelskaya and K. Lukyashchenko, Estimating soil thermal diffusivity at different water contents from easily available data on soil texture, bulk density, and organic carbon content, Biosys. Eng. **168**, 83 (2018).

[33] https://www.scientificamerican.com/article/brood-x-cicadas-are-emerging-at-last1/.

[34] Realizations of the random field were generated by inverse Fourier transforming $\hat{\phi}(k) = L\hat{C}(k)(A_k + iB_k)$, where $\hat{C}(k) = (2\pi/\lambda)/(k^2 + \lambda^{-2})^{3/2}$ is the transform of $C(r)$, L is the system size, and A_k and B_k are independent Gaussian random variables with mean 0 and variance 1. See https://cims.nyu.edu/~holmes/mathcamp/.

[35] Calculations were performed on the DAMTP HPC cluster Fawcett using a bespoke MATLAB script in task-farming mode.

[36] K. Heliövaara, R. Väisänen, and C. Simon, Evolutionary ecology of periodical insects, Trends Ecol. Evol. **9**, 475 (1994).